fractal and fractional

MDPI

Article

Vertical Distribution of Suspended Sediment Concentration in the Unsaturated Jingjiang Reach, Yangtze River, China

Meng Liu [1,2], Dong Chen [1,2,*], Hong-Guang Sun [3,4] and Feng Zhang [4]

[1] Key Laboratory of Water Cycle and Related Land Surface Processes, Institute of Geographic Sciences and Natural Resources Research, Chinese Academy of Sciences, 11A, Datun Road, Chaoyang District, Beijing 100101, China; lium.17b@igsnrr.ac.cn
[2] College of Resources and Environment, University of Chinese Academy of Sciences, Beijing 100049, China
[3] State Key Laboratory of Hydrology-Water Resources and Hydraulic Engineering, Hohai University, Nanjing 210098, China; shg@hhu.edu.cn
[4] College of Mechanics and Materials, Hohai University, Nanjing 210098, China
* Correspondence: dchen@igsnrr.ac.cn

Abstract: The Rouse formula and its variants have been widely used to describe the vertical distribution of the sediment concentration in sediment-laden flows in equilibrium. Han's formula extends the Rouse formula to non-equilibrium regimes, where the diffusive flux is still assumed to be Fickian. The turbulent flow and suspension regimes downstream of a mega-reservoir, e.g., the Three Gorges Reservoir, usually exhibit fractal and unsaturated properties, respectively. To characterize the non-Fickian dynamics of suspended sediment and the non-equilibrium regime in natural dammed rivers, this study proposes a new formula for the concentration profile of unsaturated sediment based on the Hausdorff fractal derivative advection–dispersion equation. In addition, we find that the order of the Hausdorff fractal derivative is related to the sizes of the sediment and the degrees of non-equilibrium. Compared to Rouse and Han's formulae, the new formula performs better in describing the sediment concentration profiles in the Jingjiang Reach, approximately 100 km below the Three Gorges Dam.

Keywords: Hausdorff fractal derivative; vertical distribution; suspended sediment; non-equilibrium; unsaturation

Citation: Liu, M.; Chen, D.; Sun, H.-G.; Zhang, F. Vertical Distribution of Suspended Sediment Concentration in the Unsaturated Jingjiang Reach, Yangtze River, China. *Fractal Fract.* **2023**, *7*, 456. https://doi.org/10.3390/fractalfract7060456

Academic Editor: Haci Mehmet Baskonus

Received: 20 April 2023
Revised: 18 May 2023
Accepted: 27 May 2023
Published: 2 June 2023

1. Introduction

Stream channels transport water and sediment from the upper watersheds. With the rapid socio-economic development in the middle- and lower-Yangtze River Basin, China, the authorities have constructed a series of mega-reservoirs in the upper reach. Among them, the Three Gorges Reservoir (TGR) may be the most famous one. Upstream damming regulates runoff and traps sediment, therefore significantly altering the natural flow and sediment regimes in the lower reaches [1,2], resulting in channel degradation, bed armoring, bar reshaping, streambank erosion [3–5], and eco-environmental issues [6,7].

Under the long-term influence of low-sediment-concentration flows, the riverbed will suffer from scouring, undercutting, or bank widening, and river patterns may change, which in turn affects human beings [8,9]. Before the impoundment of the TGD in 2003, the middle Yangtze River was considered a quasi-equilibrium channel with limited bed deformation and fluctuations in the suspended sediment concentration (SSC) [10]. With the completion and operation of a series of reservoirs on the main stem and tributaries of the upper Yangtze River, the lower reaches, e.g., the Jingjiang (JJ) Reach, have experienced a significant change in sediment transport regimes, mainly from quasi-equilibrium to unsaturation [9,11–13]; this change has resulted in bed scouring [14], bank collapse [4], and a decrease in the SSC [15].

Since the Schmidt diffusion theory was introduced in 1925, the vertical distribution of suspended sediment has been studied for a long time by many scholars based on various theories [16]. Notably, the Rouse equation has been widely used [17], which motivated various improvements by a number of scholars. Based on laboratory data, Van Rijn and Wang and Qian [18,19] discussed the value range of the correction parameter β, a coefficient related to the diffusion of sediment particles. Umeyaina [20] studied the vertical distribution of suspended sediment in uniform open-channel flows based on the mixing length theory. Cao et al. [21] developed a model for the vertical distribution of the SSC in open-channel flows by using the turbulent burst theory. Fu et al. [22,23] quantified the suspended sediment in solid–liquid two-phase flows with a kinetic theory-based model. Zhong et al. [24] derived a suspended sediment transport equation based on a solid–liquid two-phase flow model. All of the above studies focused on the vertical distribution of the SSC in an equilibrium state, but dammed river channels are typically not in equilibrium. Dou [25] proposed a preliminary theoretical system for non-equilibrium sediment transport. Han et al. [26] modified the Rouse formula by adding a non-equilibrium coefficient c, which represents the deviation of the vertical profiles of the SSC from the Rouse result. Ma et al. [27] improved Han's equation by reducing the number of unknown parameters from three to two.

One of the implicit hypotheses of most previous studies was Fick's first law, in which the diffusive flux is proportional to the gradient of concentration. To address the anomalous diffusion in suspension, e.g., non-local vertical jumps induced by turbulent bursts, Chen et al. [28] proposed a fractional dispersion equation for sediment suspension. Recently, researchers employed fractal derivatives to study complex fluid flows and solute transport [29–33]. Nie et al. applied both fractional and fractal derivatives to describe the anomalous diffusion of suspended sediment in many classic laboratory experiments [34–36]. Sun et al. [16] proposed a Hausdorff fractal derivative-based advection–dispersion equation (HADE) model, where the Fickian diffusive flux in the Rouse formula was replaced with a fractal derivative, rescaled using a constant diffusivity. This paper aims to extend Sun et al.'s [16] work to non-equilibrium sediment regimes and develop a novel equation that can be applied to an unsaturated reach below reservoirs, such as the Jingjiang Reach, which is approximately 100 km below the Three Gorges Dam.

2. Study Area, Data, and Methods

2.1. Study Area

The Yangtze River stands out as the third longest river in the world, and the Jingjiang (JJ) Reach (length of 347.2 km from the Zhicheng to Chenglingji gauges) is located in the middle Yangtze River. This study focuses on the sediment suspension regime in the JJ Reach from the Zhicheng (ZC) to Jianli (JL) gauges, which is approximately 243 km in length, as shown in Figure 1. ZC is approximately 100 km below the Three Gorges Dam (TGD). In addition to ZC and JL, the Shashi (SS) gauge is present in this reach and is approximately 92 km below ZC. Three tributary channels, namely, Songzikou, Taipingkou, and Ouchikou, connect the Yangtze River with Dongting Lake. Ouchikou divides the JJ Reach into upper and lower segments, and the riverbeds in these segments are composed of gravel–sand and sand, respectively [37,38].

The TGR began operation after June 2003. The initial storage level was 135 m during dry seasons, then increased to 156 m in October 2006 and 175 m in November 2008 [39]. The authorities kept building cascade dams upstream, including the Wudongde, Baihetan, Xiluodu, and Xiangjiaba reservoirs, which began operation after 2012 [1].

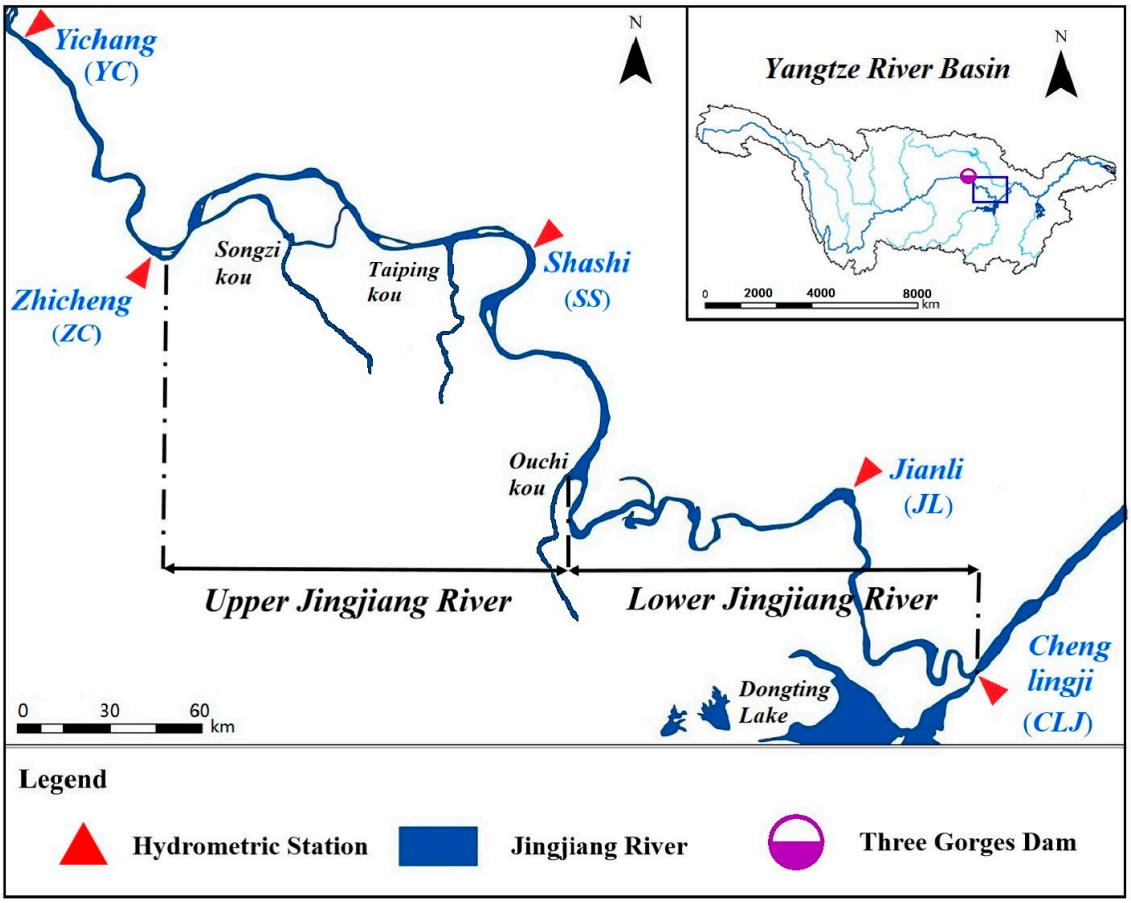

Figure 1. The Jingjiang (JJ) Reach. The gauges include Yichang (YC), Zhicheng (ZC), Shashi (SS), Jianli (JL), and Chenglingji (CLJ). The Yangtze River Basin and the location of the Three Gorge Dam (TGD) are shown in the insert. The three tributary channels, namely, Songzikou, Taipingkou, and Ouchikou, are also shown.

2.2. Data

Field survey data from the JJ Reach were provided by the Bureau of Hydrology, Changjiang Water Resources Commission, and they include flow discharge, flow velocity, water depth, sediment concentration, and size gradation of suspended sediment on vertical profiles obtained at the ZC, SS, and JL gauges. The duration of the measurement period varied at the three gauges, as shown in Table 1. There were 3–15 vertical profiles in the gauged sections and 5 or 7 observation points for each vertical profile. The Jingjiang Bureau of Hydrology formerly adopted the traditional 5-point method to record the flow velocity and sediment concentration at relative water depths of 1.0 h, 0.8 h, 0.4 h, 0.2 h, and 0.1 h in each vertical profile (h represents the local flow depth, ranging from 2.09 m to 25.7 m at the three gauges). In the periods of 2006–2007, 2010–2013, and 2015–2016, the bureau extended the 5-point method to the 7-point method by adding two more observation points, i.e., 0.5 m and 0.1 m from the riverbed [40].

Table 1. Details of the vertical profiles of SSC in the JJ Reach.

Station	Before TGR Activation	After TGD Activation	Data Details
ZC	2000–2001	2004–2021	3–15 vertical profiles per gauge; measured 1–18 times per year
SS	1981–2002		
JL	1982–2002		

2.3. Methods

2.3.1. Hausdorff Fractal Space

Many previous investigations of sediment suspension in steady and equilibrium sediment-laden flows are based on the Schmidt equation [16,28]:

$$\omega s + \varepsilon_{sy} \frac{\partial S}{\partial y} = 0 \tag{1}$$

where ω denotes the sediment settling velocity (L/T); S is the volumetric concentration of sediment; y represents the vertical distance from the streambed [L]; and ε_{sy} is the vertical component of the sediment diffusion coefficient [L^2/T]. Equation (1) indicates that the vertical distribution of the SSC in the equilibrium regime is determined by the balance between two opposite movements: downward settling and upward diffusion.

By assuming $\varepsilon_{sy} = \varepsilon_m = \kappa u_*(1 - y/h)y$ where ε_m is the fluid eddy viscosity; κ is the Von Karman constant; u_* is the shear velocity [L/T]; and h is the water depth [L]. Rouse [17] provided an analytical solution to Equation (1):

$$\frac{S}{S_*} = \left[\frac{\frac{h}{y} - 1}{\frac{h}{a} - 1}\right]^{\frac{\omega}{\kappa u_*}} \tag{2}$$

where a is a given height [L]; S_* is a reference concentration at a given height a [L] above the streambed; h is the water depth [L]; κ is the Von Karman constant; and u_* is the shear velocity [L/T]. $\omega/\kappa u_*$ is called the suspension index.

The Rouse equation adopts the passive scalar hypothesis and is therefore suitable for dilute suspension, such as in Jiangjiang cases. However, it apparently suffers from fatal deficiencies, such as zero and infinite values of concentration at the water surface and streambed, respectively. More crucially, the Rouse equation is not applicable to non-equilibrium states in which the downward settling of suspended sediment cannot be balanced by the upward turbulent diffusion in Equation (1). To address this issue, Han et al. [26] extended the suspension index to $c\omega/\kappa u_*$. Here c is called the non-equilibrium parameter, which is assumed to be a function of the ratio of the depth-averaged concentration $\overline{S}$ to the carrying capacity $\overline{S}_*$, namely $c = 1 - f\left(\frac{\overline{S}}{\overline{S}_*}\right)$ [27]. $c > 1$ and $c < 1$ represent the unsaturation and over-saturation regimes, respectively. However, the parameter c actually represents the deviation of the non-equilibrium SSC profiles from that in Equation (2). Due to the limitation of Equation (2) (e.g., lack of non-Fickian diffusion consideration, as explained in Chen et al. [28] and Nie et al. [36]), Han's equation does not always accurately express the vertical profile of the SSC, sometimes even contradicting real-world measurements [41].

Figure 2a sketches a diagram of sediment suspension with the flow depth divided into eight layers. Statistically, any particles from the bottom layer have a chance to jump to any upper layers. In equations based on Fickian law, e.g., Rouse or Han's equations, it is assumed that the turbulence-induced upward movement of particles is controlled by the Central Limit Theorem. In other words, the probability of a suspended particle jumping upward decays exponentially with the jump length [28]. However, it can be argued that non-local particle jumps are common in an open-channel flow due to the existence of coherent turbulent structures. As a more general expression, the probability of a particle moving a given distance upward decreases as a power law with an order of α ($0 < \alpha \leq 1$, where $\alpha = 1$ indicates that Fick's first law is valid).

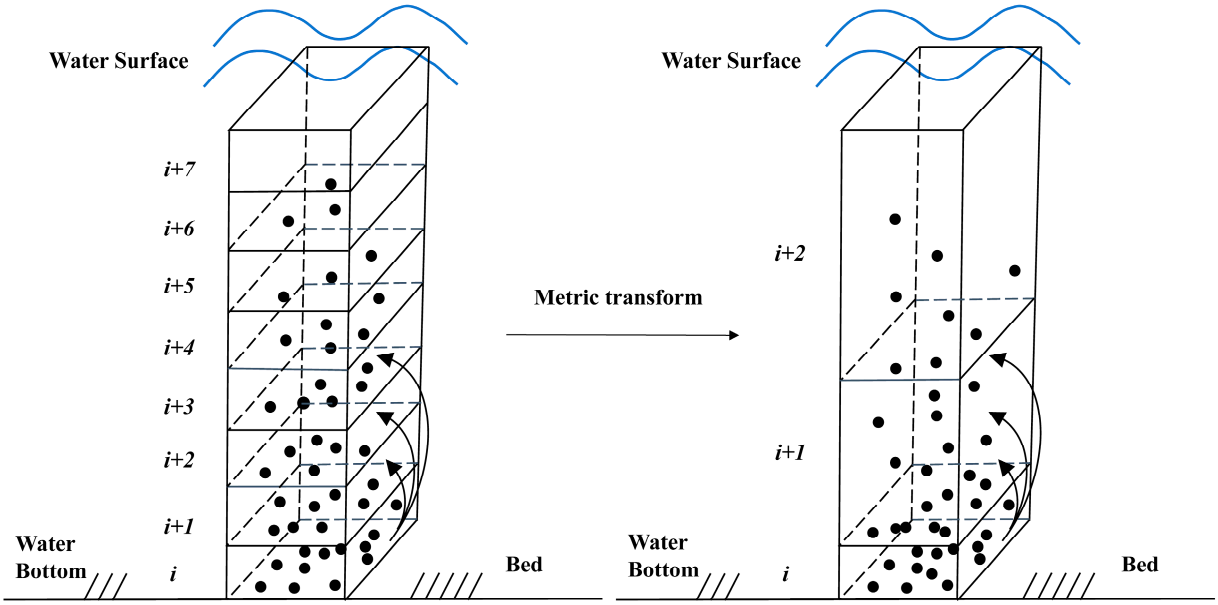

Figure 2. Abnormal diffusion in (**a**) Euclidean geometric space and (**b**) Hausdorff fractal space.

An alternative way to ensure that $\alpha \equiv 1$, i.e., Fick's first law, is always valid is to transform the Euclidean geometric space to the Hausdorff fractal space, as shown in Figure 2. The metric transformation is based on two assumptions: (a) the physical laws are invariant; and (b) the influence of anomalous fluctuations on physical behavior is equivalent to that of the fractal space transform [42]. With these assumptions, the Hausdorff fractal derivative can be expressed as

$$\frac{\partial f(y)}{\partial y^{\gamma}} = \lim_{y_1 \to y} \frac{f(y_1) - f(y)}{y_1^{\gamma} - y^{\gamma}} \tag{3}$$

where γ is called the Hausdorff space coefficient, which is related to the fractal dimension of the space.

2.3.2. Hausdorff Fractal Deviation for Non-Equilibrium SSC Vertical Profile

To address the anomalous diffusion and the non-equilibrium regime in the JJ Reach after the TGR impoundment, we propose a Hausdorff fractal derivative, as follows.

First, we modify the Schmidt equation, as follows:

$$\omega s + \varepsilon_{sy} \frac{\partial s}{\partial y} = q_{sy} \tag{4}$$

where q_{sy} is the vertical net sediment flux at the position y [L/T]. Following Chen et al., 2013 [28], we substitute the depth-variable ε_{sy} for a depth-averaged or depth-constant ε_s:

$$\bar{\varepsilon}_{sy} = \frac{\int_{0.05h}^{h} \kappa u_* (1 - y/h) y dy}{0.95h} = \frac{209 \kappa u_* h}{1200} \tag{5}$$

and rearrange Equation (4) as:

$$\frac{\partial s}{\partial y} + \frac{\omega}{\varepsilon_s} s = q_{ss} \tag{6}$$

where $q_{ss} = q_{sy}/\varepsilon_s$.

It is assumed that q_{ss} linearly changes with the water depth, reaching a value of zero at the bed and a maximum at the water surface:

$$q_{ss} = q_s(y/h) \tag{7}$$

where q_s is constant and $q_s = q_{ss}$ when $y = h$.

Equation (6) is a non-homogeneous linear first-order differential equation, and its general solution can be expressed as:

$$\frac{S}{S_a} = e^{-\frac{\omega}{\varepsilon_s}(y-a)}\left(\int_a^y q_s\left(\frac{y}{h}\right)e^{\frac{\omega}{\varepsilon_s}(y-a)} + C\right) \tag{8}$$

where C is an integral constant.

We set:

$$\int_a^y q_s\left(\frac{y}{h}\right)e^{\frac{\omega}{\varepsilon_s}(y-a)} = \int_a^y Dye^{\frac{\omega}{\varepsilon_s}(y)} \tag{9}$$

where $D = \frac{q_s e^{\frac{\omega}{\varepsilon_s}(-a)}}{h}$

According to the partial integration method:

$$\int_a^y Dye^{\frac{\omega}{\varepsilon_s}(y)} = \left(\frac{\varepsilon_s}{\omega}\right)^2 D\left(e^{\frac{\omega}{\varepsilon_s}(y)}\left(\frac{\omega}{\varepsilon_s}y - 1\right) - e^{\frac{\omega}{\varepsilon_s}(a)}\left(\frac{\omega}{\varepsilon_s}a - 1\right)\right) \tag{10}$$

We express $e^{\frac{\omega}{\varepsilon_s}(y)} = \kappa \cdot e^{\frac{\omega}{\varepsilon_s}(a)}$ using first-order Tayler's formula and $\kappa = 1 + \frac{\omega}{\varepsilon_s}(y-a)$.

Since the suspended sediment in the JJ Reach is mainly composed of wash-load with particle size $d < 0.062$ mm [43], therefore $\omega << \varepsilon_s$ and $\kappa \approx 1$. For instance, the data on 2 August 2013 at JL gauge in the near-surface zone (>0.8 h), where d = 0.022 mm, ω = 0.0003 m/s, ε_s = 0.135 u/h, and κ = 1.002. Equation (10) can be approximated as:

$$\int_a^y Dye^{\frac{\omega}{\varepsilon_s}(y)} \cong \frac{\overline{q}_s}{h}\frac{\varepsilon_s}{\omega}(y-a) \tag{11}$$

By substituting Equation (11) into Equation (8), we obtain:

$$\frac{S}{S_a} = e^{-\frac{\omega}{\varepsilon_s}(y-a)}\left(\frac{q_s}{h}\frac{\varepsilon_s}{\omega}(y-a) + C\right) \tag{12}$$

According to the boundary condition, $s = s_a$ when $y = a$; therefore, $C = 1$. Equation (12) becomes:

$$\frac{S}{S_a} = e^{-\frac{\omega}{\varepsilon_s}(y-a)}\left(\frac{q_s}{h}\frac{\varepsilon_s}{\omega}(y-a) + 1\right) \tag{13}$$

Equation (13) describes the vertical distribution of the non-equilibrium SSC, and its Hausdorff fractal derivative is:

$$\frac{S}{S_a} = e^{-\frac{\omega}{\varepsilon_s}(y^\gamma - a^\gamma)}\left(\frac{q_s}{h}\frac{\varepsilon_s}{\omega}(y^\gamma - a^\gamma) + 1\right) \tag{14}$$

where γ is the Harsdorf fractal coefficient and $0 < \gamma \leq 1$.

3. Results

3.1. Comparison of Formulae in Describing Vertical Sediment Profiles

Numerous formulae can be used when simulating the vertical distribution of the SSC in open channel flows. In this study we validate the applicability of Equation (14) by comparing the calculations to the measurements with various flow discharges and particle sizes at the ZC, SS, and JL gauges in the JJ reach.

In Figure 3, we compare the performance of three formulae, namely, Rouse equation, Han's equation, and Equation (14), in simulating the real-world vertical distribution of the SSC in the JJ Reach. The measured data in Figure 3a,b are from the ZC gauge; the data in

Figure 3c,d are from the SS gauge; and the data in Figure 3e,f are from the JJ gauge. All the data are from field surveys conducted by the Bureau of Hydrology, Changjiang Water Resources Commission, with particle sizes ranging from 0.003 to 0.06 mm and local flow depths between 10 and 24 m.

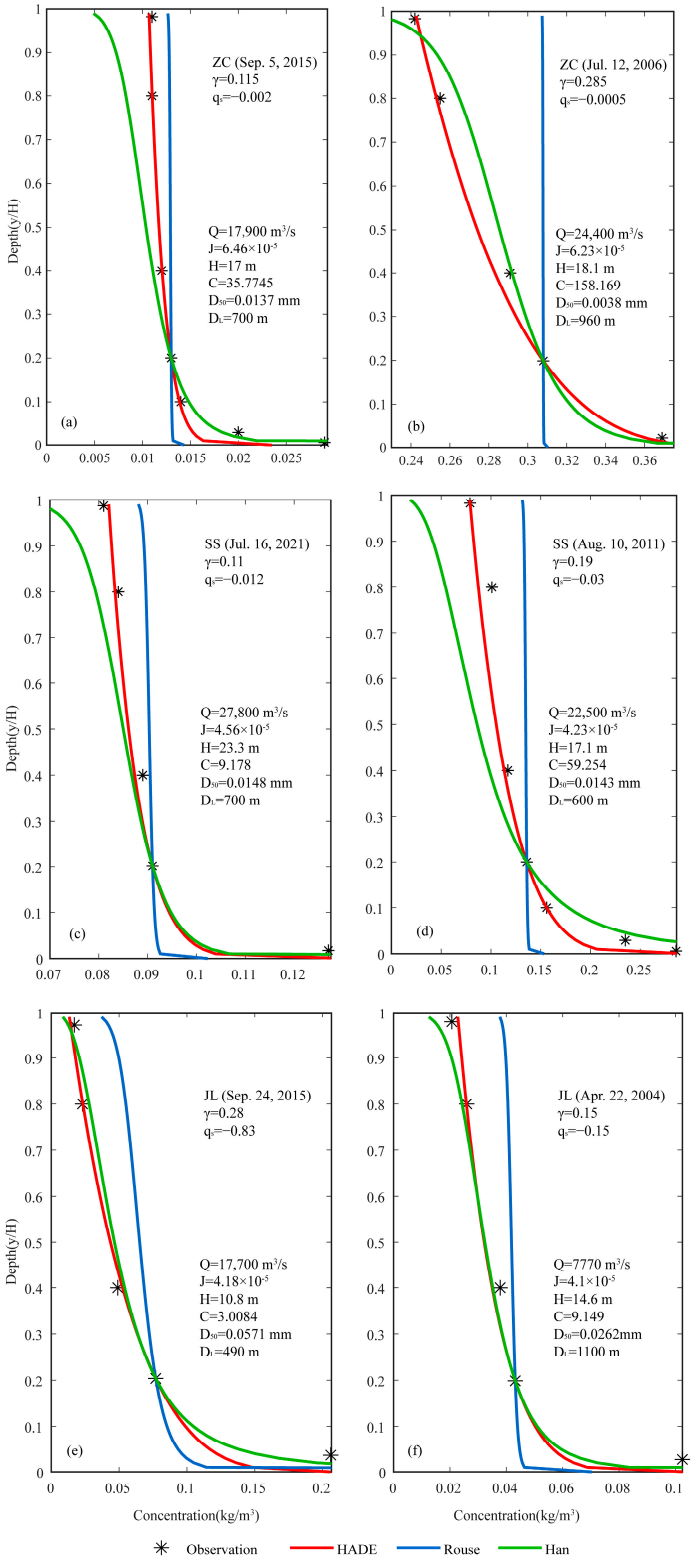

Figure 3. Results of the three formulae in describing the vertical distribution of sediment suspension. The Von Karman constant $\kappa = 0.4$, and the reference height $a = 0.2$ h.

Figure 3 indicates that Equation (14) performs the best in simulating the vertical distribution of suspended sediment under a non-equilibrium sediment regime. Due to the relatively high sediment concentration in the near-bed area and the low sediment concentration in the upper water layers, there is a remarkable "tailing phenomenon" in the near-bed zone (<0.2 h) of the vertical profiles in non-equilibrium sediment regimes, for which the Rouse formula is not at all applicable. Han's formula can better describe the tails; however, it sometimes underestimates the sediment concentration in the upper water layers, especially for finer particles in the near-surface zone (>0.8 h). This limitation is very likely because Han's formula neglects the anomalous diffusion of suspended sediment. As indicated by Chen et al. [28], turbulent bursts may sweep the bed, grab sediment particles, and non-locally jump to the upper water layers. The orders of the Hausdorff fractal derivative in Figure 3 are as low as 0.1–0.3, indicating that the upward anomalous diffusion ability in the non-equilibrium regime might be stronger than that quasi-equilibrium conditions.

3.2. Parameters That Influence γ

We analyzed the parameters that can affect the order of the Hausdorff fractal derivative γ. Figure 4 shows the relationship between γ and the particle size d. We divided the data into four periods, namely, 1980–2002: the pre-TGR period; 2003–2008: the cofferdam period; 2009–2012: TGR operation; and 2013–2021: the operation period for cascade reservoirs.

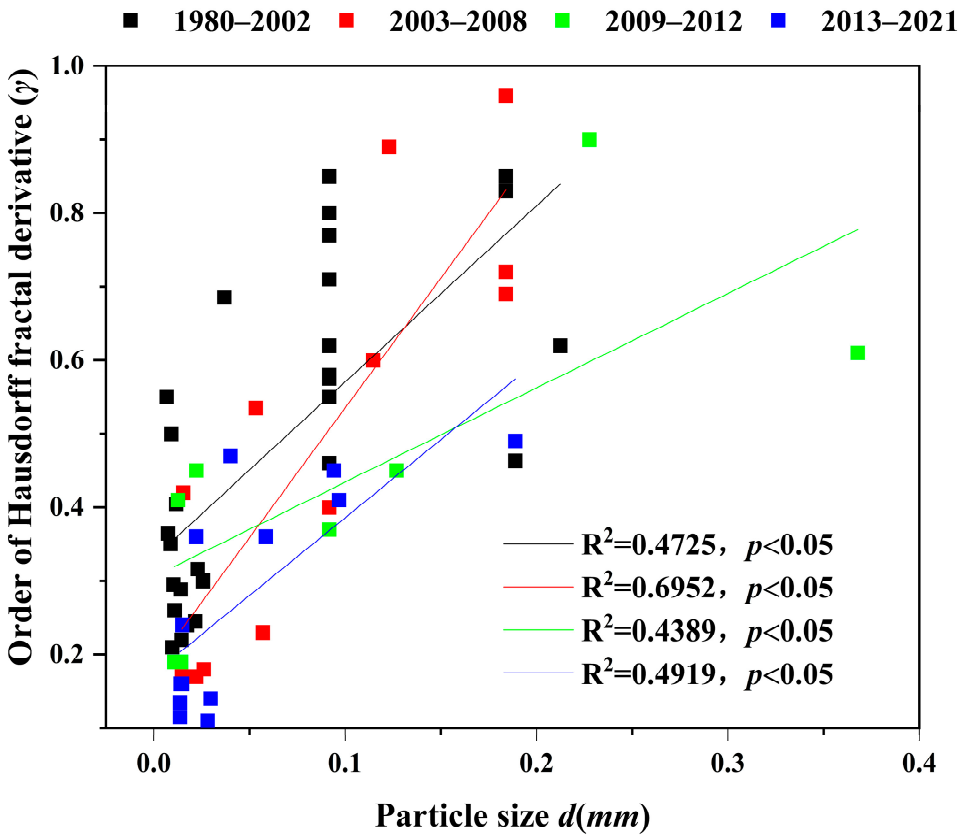

Figure 4. The relationship between the order of the Hausdorff fractal derivative γ and the particle size d.

The fitting curves in Figure 4 indicate that the order of the Hausdorff fractal derivative γ increases with particle size d in all four periods. The small γ values for fine particles indicate that these particles are more likely to make longer vertical jumps in turbulent bursts, resulting in super-diffusion in Euclidean geometric space, which needs to be radically

transformed into Hausdorff fractal space to validate Fick's first law. In contrast, the coarser particles are more controlled by gravitational settling and less affected by turbulent bursts.

In addition to particle size d, the degree of non-equilibrium should also be an important parameter that influences the vertical profiles, as discussed above. In this study, we calculated the degree of non-equilibrium ξ using the following formula:

$$\xi = \frac{\overline{S} - \overline{S}_*}{\overline{S}_*} \tag{15}$$

where $\overline{S}$ is the depth-averaged concentration and $\overline{S}_*$ is the depth-averaged concentration before the impoundment of the TGD, which is equivalent to the carrying capacity under equilibrium conditions. According to the long-term data in the pre-TGD period, the JJ Reach was in a quasi-equilibrium state, i.e., the ξ value was close to 0. Negative and positive ξ values indicate unsaturation and supersaturation regimes, respectively. The calculation of the carrying capacity is based on Zhang's formula [44].

Figure 5 indicates that the order of the Hausdorff fractal derivative γ decreases as the absolute value of the degree of non-equilibrium increases, approaching -1. Figure 5 also indicates that the higher non-equilibrium degrees are usually associated with smaller particle size d. The smallest value of γ occurred when $\xi = -0.973$ and $d = 0.028$ mm. Again, this trend may be related to the enhanced non-local particle jumps in the non-equilibrium regime.

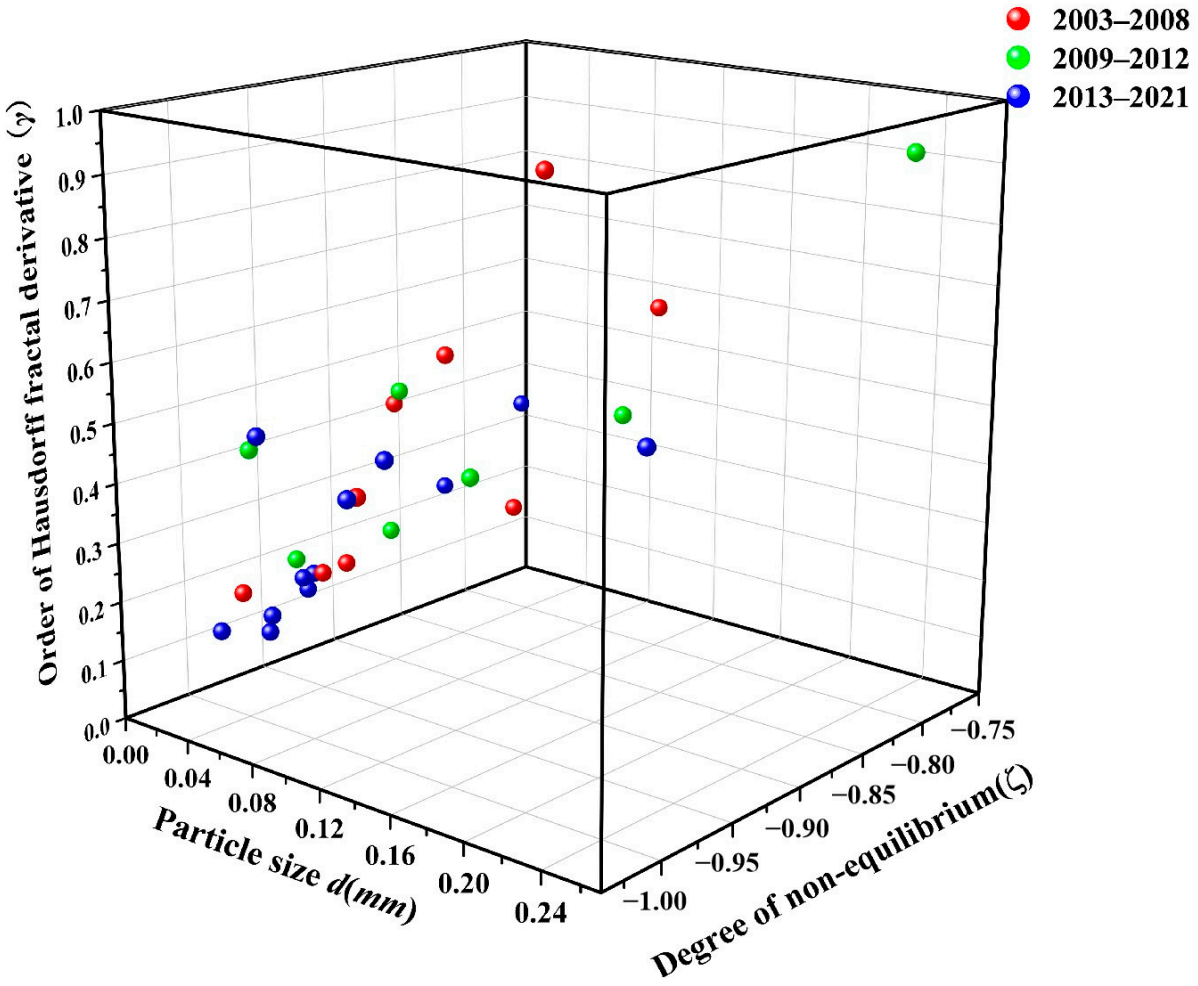

Figure 5. The relationships between the order of the Hausdorff fractal derivative, the degree of non-equilibrium, and the particle size.

Equation (16) provides the best linear fit:

$$\gamma = 2.87599d + 0.05738\xi + 0.236 \quad R^2 = 0.66001 \quad p < 0.05 \tag{16}$$

4. Discussion

Sensitivity Analysis

In Figure 6, we evaluated the sensitivity of the vertical distribution of the SSC to the selection of γ values. The case chosen here is the field measurement from the ZC gauge on 12 July 2006, for which d_{50} = 0.0038 mm. The best fit in Figure 6 is obtained with γ = 0.3. Figure 6 indicates that a small γ, e.g., 0.1, in Equation (14) will lead to underestimation of the concentration in the near-bed zone and overestimation in the upper water layers. In contrast, if γ is too large, e.g., 0.6, in Equation (14), the concentration in the near-bed zone will be overestimated, with underestimation in the upper water layers. The estimated concentration values at 0.8 h will decrease to 36% and 88% of the measured values (0.255 kg/m^3) for γ = 0.6 and γ = 0.4, respectively. This indicates that the calculated profiles for the fine particles are sensitive to γ values.

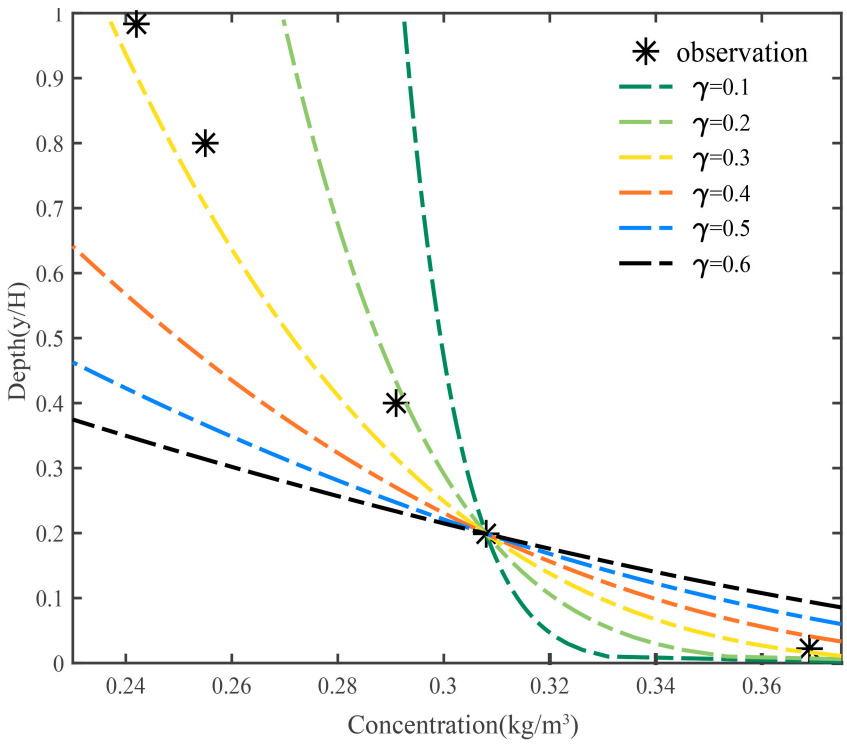

Figure 6. The sensitivity of the vertical profiles of the SSC to various γ values (calculated using Equation (13)). The other parameters are κ = 0.4, ε_s = 0.13, ω = 1.45 × 10^{-5}, u_* = 0.105, q_s = −0.0005.

When the downward settling of the suspended sediment cannot be balanced by upward turbulent diffusion, a net sediment flux q_s will be generated in the vertical direction. Figure 7 shows that the vertical distribution of the SSC is also sensitive to the vertical net sediment flux q_s. When the absolute values of q_s approach zero, the sediment regime is in quasi-equilibrium, the concentration in the near-bed zone is underestimated, and the concentration in the upper water layers is overestimated. When q_s = −0.0005, Equation (14) becomes nearly identical to the Rouse formula. In Figure 6, q_s = −0.0005 provides the best fit to the measurements at both 0.8 h and 1.0 h. However, when q_s is taken as −0.0006 and −0.0008, the estimated concentration values at 0.8 h are reduced to 94% and 86% of the measured value (0.255 kg/m^3), respectively.

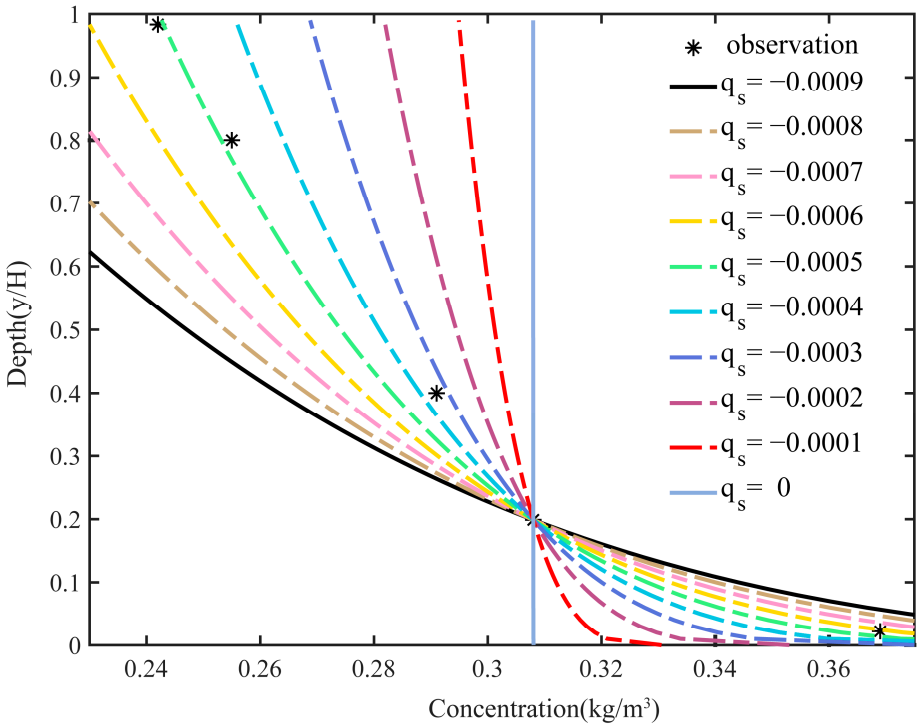

Figure 7. The SSC profiles with various vertical net sediment flux q_s (calculated using Equation (13)). The other parameters are $\kappa = 0.4$, $\varepsilon_s = 0.13$, $\omega = 1.45 \times 10^{-5}$, $u_* = 0.105$, $\gamma = 0.3$.

5. Conclusions

Due to the operations of a series of mega-reservoirs in the upper reachof the Yangtze River, the sediment regime in the JJ Reach has changed dramatically, displaying fractal and unsaturated characteristics. Based on the Hausdorff fractal derivative, which transforms the Euclidean geometric space to the fractal space, we propose a new equation to describe the vertical distribution of the SSC in the JJ Reach. The new equation performs better than the Rouse and Han's formulae, avoiding their boundary-value deficiencies. In addition, we find that the order of the Hausdorff fractal derivative γ is related to the sizes of sediment particles and the degrees of non-equilibrium. We still need further data from field measurements and experiments to obtain a more robust prediction of γ in the future.

Author Contributions: M.L., conceptualization, methodology, validation, visualization, writing—original draft, writing—review and editing; D.C., supervision, formal analysis, funding acquisition, writing—review and editing; H.-G.S., supervision, writing—review and editing; F.Z., methodology, writing, and editing. All authors have read and agreed to the published version of the manuscript.

Funding: This study was supported by the National Key Research and Development Program of China (2022YFC3203903) and the National Natural Science Foundation of China (No. 52279077).

Data Availability Statement: The data used in this work are available upon request.

Conflicts of Interest: The authors declare no conflict of interest.

References

1. Yan, H.C.; Zhang, X.F.; Xu, Q.X. Unprecedented sedimentation in response to emerging cascade reservoirs in the upper Yangtze River Basin. *Catena* **2022**, *209*, 105833. [CrossRef]
2. Guo, X.H.; Qu, G.; Liu, Y.; Liu, X.Y. Sediment transport of different particle size groups in the downstream channel after operation of the Three Gorges Project. *J. Lake Sci.* **2020**, *32*, 564–572. [CrossRef]
3. Li, X.; Xia, J.; Li, J.; Zhou, M. Adjustments in reach-scale bankfull geometry of a braided reach undergoing contrasting channel evolution processes. *Arab. J. Geosci.* **2019**, *12*, 535. [CrossRef]

4. Xia, J.; Deng, S.; Zhou, M.; Lu, J.; Xu, Q. Geomorphic response of the Jingjiang Reach to the Three Gorges Project operation. *Earth Surf. Process. Landf.* **2017**, *42*, 866–876. [CrossRef]
5. Petts, G.E.; Gurnell, A.M. Dams and geomorphology: Research progress and future directions. *Geomorphology* **2005**, *71*, 27–47. [CrossRef]
6. Mccartney, M.P.; Shiferaw, A.; Seleshi, Y. Estimating environmental flow requirements downstream of the Chara Chara weir on the Blue Nile River. *Hydrol. Process.* **2009**, *23*, 3751–3758. [CrossRef]
7. Wohl, E.; Lane, S.N.; Wilcox, A.C. The science and practice of river restoration. *Water Resour. Res.* **2015**, *51*, 5974–5997. [CrossRef]
8. Kamboj, V.; Kamboj, N.; Sharma, A.K. A review on general characteristics, classification and degradation of river systems. *Environ. Degrad. Causes Remediat. Strateg.* **2020**, *1*, 47–62.
9. Yang, X.H.; Xiong, H.B.; Li, D.F.; Li, Y.T.; Hu, Y. Disproportional erosion of the middle-lower Yangtze River following the operation of the Three Gorges Dam. *Sci. Total Environ.* **2023**, *859*, 160264. [CrossRef]
10. Huang, H.Q.; Deng, C.; Nanson, G.C.; Fan, B.; Liu, X.; Liu, T.; Ma, Y. A test of equilibrium theory and a demonstration of its practical application for predicting the morphodynamics of the Yangtze River. *Earth Surf. Process. Landf.* **2014**, *39*, 669–675. [CrossRef]
11. Zuo, S.; Yang, C.; Fu, G.; Xie, H. Variation of water and sediment flux and its influence on the Yangtze River Estuary. *Mar. Geol. Front.* **2022**, *38*, 56–64. [CrossRef]
12. Zuo, S.H.; Zhang, N.C.; Li, B.; Yang, H. Dynamics reasons and temporal-spatial variations of suspended sediment condition in the sea area of Yangshan deep-water harbor. *J. East China Norm. Univ.* **2009**, *3*, 72–82.
13. Li, Y.; Sun, Z.; Deng, J. A Study on Riverbed Erosion Downstream from the Three Gorges Reservoir. *J. Basic Sci. Eng.* **2003**, *11*, 283–295. (In Chinese)
14. Liu, X.Q. Research on riverbed adjustment response of jingjiang reach under the change of flow and sediment. *Appl. Ecol. Environ. Res.* **2017**, *15*, 911–922. [CrossRef]
15. Yang, S.L.; Milliman, J.D.; Xu, K.H.; Deng, B.; Zhang, X.Y.; Luo, X.X. Downstream sedimentary and geomorphic impacts of the Three Gorges Dam on the Yangtze River. *Earth-Sci. Rev.* **2014**, *138*, 469–486. [CrossRef]
16. Sun, H.G.; Nie, S.Q.; Packman, A.I.; Zhang, Y.; Chen, D.; Lu, C.P.; Zheng, C.M. Application of Hausdorff fractal derivative to the determination of the vertical sediment concentration distribution. *Int. J. Sediment Res.* **2023**, *38*, 12–23. [CrossRef]
17. Rouse, H. Modern Conceptions of the Mechanics of Turbulence. *Trans. Am. Soc. Civ. Eng.* **1937**, *102*, 463–505. [CrossRef]
18. Rijn, L. Sediment Transport, Part II: Suspended Load Transport. *J. Hydraul. Eng.* **1984**, *110*, 1613–1641. [CrossRef]
19. Wang, Z.Y.; Qian, N. Experiment study of two-phase turbulent flow with hyper concentration of coarse particles. *Chin. Sci.* **1984**, *8*, 766–773. (In Chinese)
20. Umeyaina, M. Vertical Distribution of Suspended Sediment in Uniform Open-Channel Flow. *J. Hydraul. Eng.* **1992**, *118*, 936–941. [CrossRef]
21. Cao, Z.X. Turbulent bursting-based sediment entrainment function. *J. Hydraul. Eng.* **1997**, *123*, 233–236. [CrossRef]
22. Fu, X.; Wang, G.; Shao, X. Vertical Dispersion of Fine and Coarse Sediments in Turbulent Open-Channel Flows. *J. Hydraul. Eng.* **2005**, *131*, 877–888. [CrossRef]
23. Fu, X.D.; Wang, G.Q. Analysis on the factors affecting the vertical concentration distribution of fine sediment. *J. Hydrodyn.* **2004**, *19*, 231–239. (In Chinese)
24. Zhong, D.; Wang, G.; Sun, Q. Transport Equation for Suspended Sediment Based on Two-Fluid Model of Solid/Liquid Two-Phase Flows. *J. Hydraul. Eng.* **2011**, *137*, 530–542. [CrossRef]
25. Dou, G.R. Suspended sediment movementand calculation of erosion and deposition in tidal flow. *J. Hydraul. Eng.* **1963**, *4*, 13–24. (In Chinese)
26. Han, Q.W.; Chen, X.J.; Xue, X.C. On the vertical distribution of sediment concentration in non-equilibrium transportation. *Adv. Water Sci.* **2010**, *21*, 512–523. (In Chinese)
27. Ma, Z.; Guo, Q.; Guan, J.; Le, M. Non-equilibrium concentration profile formulas of suspended sediment and their preliminary applications. *Int. J. Sediment Res.* **2022**, *37*, 505–513. [CrossRef]
28. Chen, D.; Sun, H.G.; Zhang, Y. Fractional dispersion equation for sediment suspension. *J. Hydrol.* **2013**, *491*, 13–22. [CrossRef]
29. Liang, Y.; Dou, Z.; Zhou, Z.; Chen, W. Hausdorff derivative model for characterization of non-fickian mixing in fractal porous media. *Fractals* **2019**, *27*, 1950063. [CrossRef]
30. Zhang, Y.; Zhou, D.B.; Yin, M.S.; Sun, H.G.; Wei, W.; Li, S.Y.; Zheng, C.M. Nonlocal-transport models for capturing solute transport in one-dimensional sand columns: Model review, applicability, limitations, and improvement. *Hydrol. Process.* **2020**, *34*, 5104–5122. [CrossRef]
31. Christov, I.C. Soft hydraulics: From Newtonian to complex fluid flows through compliant conduits. *J. Physics. Condens. Matter* **2021**, *34*, 063001. [CrossRef]
32. Al-Raeei, M. Morse potential specific bond volume: A simple formula with applications to dimers and soft–hard slab slider. *J. Phys. Condens. Matter* **2022**, *34*, 284001. [CrossRef] [PubMed]
33. Wei, Y.; Rame, E.; Walker, L.M.; Garoff, S. Dynamic wetting with viscous newtonian and non-newtonian fluids. *J. Phys. Condens. Matter* **2009**, *21*, 464126. [CrossRef]
34. Nie, S.; Sun, H.G.; Zhang, Y.; Zhou, L.; Chen, D. A fractal derivative model to quantify bed-load transport along a heterogeneous sand bed. *Environ. Fluid Mech.* **2020**, *20*, 1603–1616. [CrossRef]

35. Nie, S.; Sun, H.; Liu, X.; Ze, W.; Xie, M. Fractal derivative model for the transport of the suspended sediment in unsteady flows. *Therm. Sci.* **2018**, *22* (Suppl. S1), 109–115. [CrossRef]
36. Nie, S.; Sun, H.G.; Zhang, Y.; Chen, D.; Wen, C.; Chen, L.; Sydney, S. Vertical Distribution of Suspended Sediment under Steady Flow: Existing Theories and Fractional Derivative Model. *Discret. Dyn. Nat. Soc.* **2017**, *2017*, 5481531. [CrossRef]
37. Meirong, Z.; Junqiang, X.; Shanshan, D.; Yu, M. Longitudinal variation of channel evolution along the middle Yangtze River after the operation of the Three Gorges Project. *J. Lake Sci.* **2023**, *35*, 642–649. [CrossRef]
38. Bureau of Hydrology, Changjiang Water Resources Commission. *Analysis on Characteristics of Flow and Sediment Characteristics, Reservoir Sedimentation and Downstream Channel of the Three Gorges Reservoir in 2018*; Wuhan Bureau of Hydrology, Changjiang Water Resources Commission: Wuhan, China, 2019. (In Chinese)
39. Ren, S.; Zhang, B.; Wang, W.; Yuan, Y.; Guo, C. Sedimentation and its response to management strategies of the Three Gorges Reservoir, Yangtze River, China. *Catena* **2021**, *199*, 105096. [CrossRef]
40. He, L.; Chen, D.; Zhang, S.; Liu, M.; Duan, G. Evaluating Regime Change of Sediment Transport in the Jingjiang River Reach, Yangtze River, China. *Water* **2018**, *10*, 329. Available online: https://www.mdpi.com/2073-4441/10/3/329 (accessed on 15 March 2018). [CrossRef]
41. He, L.; Chen, D.; Duan, G.L.; Peng, Y.M. Study on vertical distribution of suspended sediment concentration in the Jingjiang reach downstream the Three Gorges Dam. *J. Sediment Res.* **2020**, *45*, 27–32. (In Chinese)
42. Chen, W. Time-space fabric underlying anomalous diffusion. *Chaos Solitons Fractals* **2006**, *28*, 923–929. [CrossRef]
43. Zhou, Y.; Li, Z.; Yao, S.; Shan, M.; Guo, C. Case Study: Influence of Three Gorges Reservoir Impoundment on Hydrological Regime of the Acipenser sinensis Spawning Ground, Yangtze River, China. *Front. Ecol. Evol.* **2021**, *9*, 624447. [CrossRef]
44. Zhang, S.; Chen, D.; Chen, L.; Chen, X.; He, L. Using sediment rating parameters to evaluate the changes in sediment transport regimes in the middle yellow river basin, china. *Hydrol. Process.* **2019**, *33*, 2481–2497. [CrossRef]